Engineering and Technology Journal
Journal homepage: https://etj.uotechnology.edu.iq

Structural Behavior of Ultra-High-Performance Concrete Beams Under Flexural and Shear Action: A Review

Adil M. Jabbar *, Mohammed J. Hamood, Dhiyaa H. Mohammed

Civil Engineering Dept., University of Technology-Iraq, Alsina'a Street, 10066 Baghdad, Iraq.
*Corresponding author Email: adilmahdi@uowasit.edu.iq

HIGHLIGHTS

- The use of steel fibers in UHPC cannot fully substitute steel reinforcement bars that compensate for concrete weakness in tension.
- Using steel fibers in concrete can partially replace shear reinforcement due to the enhancement of shear resistance.
- Since the tensile strength of UHPC is relatively high and cannot be ignored; therefore, it is considered in the analysis and design approach of UHPC members.
- The very high compressive strength of UHPC leads to the design of structural members with smaller sizes and lightweight than the NSC or HSC under the same loading.

ARTICLE INFO

Handling editor: Wasan I. Khalil

Keywords:
Structural behavior; UHPC; Flexural analysis
Flexural design; shear analysis

ABSTRACT

Ultra-high performance concrete (UHPC) has a higher tensile strength than conventional concrete by about 6-times, besides a compressive strength greater than 150 MPa. It also exhibits linear and non-linear behavior on loading because of strain hardening and strain softening in compression and tension. Therefore, the effect of these mechanical properties can reflect in the beam behavior produced by UHPC. This paper deals with the methods and approaches adopted by some guidelines and recommendations that transact with the analysis and design of UHPC beams. The prevalent style of the methods is based on the equilibrium of the beam's section for the induced forces above the neutral axis, which represents the compression forces in concrete, and below the neutral axis, which designates the tensile forces in longitudinal rebars and that one in concrete. Since the tensile strength of UHPC is relatively high and cannot be ignored; therefore, it is considered in the analysis and design approach. The flexural capacity depends on the induced moment due to these forces. The structural analysis of UHPC depends on the stress-strain relationship in compression and tension. The linear portion of compression relation continues to about 80% of the compressive strength; therefore, it is considered in the analysis and design process.

1. Introduction

The design of reinforced concrete beams for flexural and axial force is conventionally performed by considering the linear behavior of the stress-strain diagram assuming elastic behavior only. Also, it is expressed that the plane sections remain plane after bending distortion and considering a strict bond between concrete and reinforcing bars. Furthermore, the straight portion of the compression stress-strain curve is considered in the analysis and design of the beams, whereas concrete under the neutral axis is neglected [1]. These aspects represent the method of analysis and design of NSC and HSC, as illustrated in Figure 1.

In NSC and HSC, steel rebars are usually used to compensate for the weakness of concrete, while concrete compression strength is considered in the analysis and design process. Abdulsada et al. [2] found that the concrete compression strength significantly influenced the first cracking load, where increasing compression strength raised the cracking moment. In HSC, the authors stated that the low reinforcement ratio was less influence on the working load.

http://doi.org/10.30684/etj.2021.131102.1003
Received 10 August 2021; Accepted 11 November 2021; Available online 22 June 2022
2412-0758/University of Technology-Iraq, Baghdad, Iraq

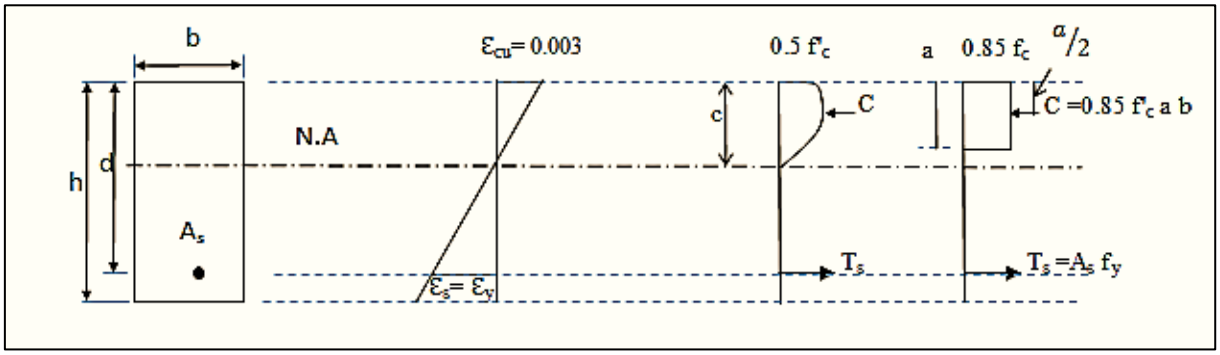

Figure 1: Stress and Strain in Rectangular Cross-Section Beam with Conventional Concrete

The incorporation of fibers in concrete has many effects on the structural behavior of concrete. They increase the tensile strength to approximately (4-8) times that of NSC. Also, it permits strain hardening and strain softening in tensile action and slightly in compression action. Thus, the concrete tensile strength does not ignore in the case of using steel fibers. ACI 544.4R [3] adopts the flexural analysis of fibrous concrete beams performed by Henger and Doherty and other researchers in a similar approach to the ACI ultimate strength design method. The method takes into consideration the tensile strength initiated by fibrous concrete. Thus, the maximum tensile capacity of the beam consists of the tensile strength of reinforcing bars and fibrous concrete, as illustrated in Figure 2.

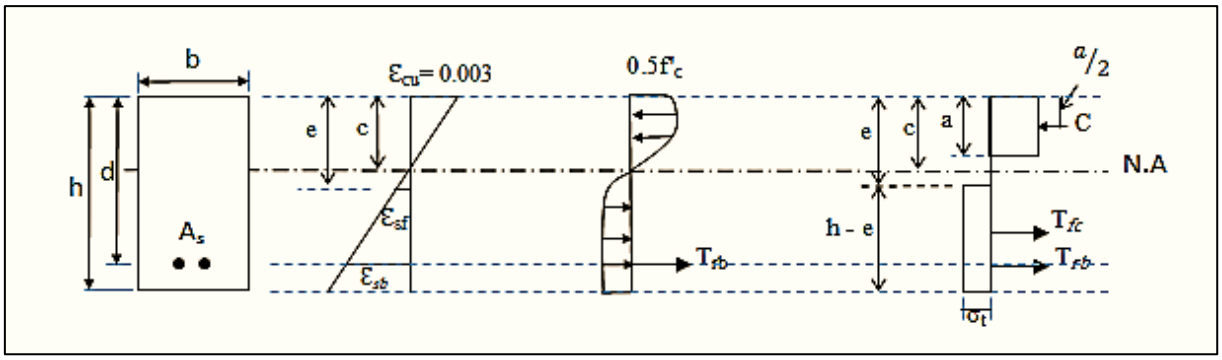

Figure 2: Compressive and Tensile Stress and Strain in Fibrous Concrete

The additional value of e represents the distance between compression concrete fibers and the starting of considered tensile strength. It can be calculated by proportionality of strains as follows:

$$\frac{e}{\varepsilon_{sf}+0.003} = \frac{c}{0.003} \qquad \text{and,} \quad e = c\,(\varepsilon sf + 0.003) / 0.003 \tag{1}$$

The nominal moment capacity of a singly reinforced fibrous concrete beam is then calculated by equilibrium conditions as follows:

$$Mn = As\ fy\ (d-\frac{a}{2}) + \frac{\sigma t}{2} b(h-e)(h+e-a) \tag{2}$$

$$\sigma t = 0.00772\ (\frac{lf}{df}) V_f\ \alpha_b \qquad (\text{in MPa}) \tag{3}$$

In which σ_t is the equivalent tensile stress in fibrous concrete. The factor 0.00772 is responsible for the bond stress of fibers in MPa. The α_b is a bond efficiency of fiber and ranges between (1.0-1.2). In the above analysis, the maximum concrete strain at compression is 0.003. At the same time, many studies, referred to them by ACI 544.4R, considered other values for maximum concrete compression strain, such as 0.0033 and 0.0035 for 1% volume fraction of fibers and 0.004 for 3% volume fraction of fibers.

The design of bending strength in ACI 318 [4] is multiplied by strength reduction factors, whereas load factors magnify the applied loads. In fibrous concrete, the contribution of tensile strength is about (5-15) % of the resisting moment, which can be considered a significant contribution but not a meaningful part. Therefore, a strength reduction factor for reinforcing bars to use in design strength is the same as that used for NSC, which is (ϕ = 0.9), and a smaller ϕ for tension contribution can be considered [3].

The use of steel fibers in reinforced concrete (SFRC) cannot fully substitute steel reinforcement bars which compensate for the weakness of concrete in tension. Although using fibers can improve the tensile strength in SFRC and UHPC, this improvement is just a few. On the other hand, using steel fibers in concrete can partially replace shear reinforcement due to the enhancement of shear resistance [5].

Rjoub [5] proposed a set of equations to predict the moment capacity of SFRC beams. The moment equation consists of two divisions. The first is for a moment due to steel reinforcement bars (M_c), and the other is for a moment due to the increment in modulus of rupture resulting from incorporating steel fibers in NSC (M_f). These equations are as follows:

$$M_f = 0.167\ \Delta fr\ b\ h^2 \tag{4}$$

$$M_c = As\ fy\ (\ d - \frac{a}{2}\ ) \tag{5}$$

$$M_n = M_f + M_c \tag{6}$$

$$a = \frac{A_s f_y}{0.85 f'_c b} \tag{7}$$

$$\Delta fr\ = 0.61\ V_f\ (\frac{l_f}{d_f})\ fr \quad \text{for linear regression} \tag{8}$$

$$\Delta fr\ = [0.21\ V_f^2 (\frac{l_f}{d_f})^2 + 0.36\ V_f\ (\frac{l_f}{d_f})\ ]\ f_r \quad \text{for non-linear regression} \tag{9}$$

Where fr is the modulus of rupture of plain concrete, as it is used by ACI 318M-05[4]:

$$f_r = 0.7\ \lambda\ \sqrt{f'_c} \tag{10}$$

Rjoubs' equations provided accurate results for NSC and underestimated the moment capacity of HSC with fibers.

Oh [6] also studied the flexural behavior of fibrous reinforced concrete beams and derived a set of equations for calculating the flexural strength of fibrous reinforced concrete. He assumed that the flexural strength consists of matrix strength and fiber strength, as follows:

$$\sigma_{ct} = \sigma_{mt}\ V_m + \sigma_t\ V_f \tag{11}$$

σ_{ct} is the flexural strength of FRC, σ_{mt} is the matrix flexural strength, σt is the fiber strength in MPa, V_m is the matrix volume = 1-V_f, and V_f is the fiber volume fraction.

Three parameters related to fibers were adopted in Ohs' equations. These were the orientation, length, and bonding features of fibers. These parameters are applied to predict the fiber strength as follows:

$$\sigma_{ct} = \sigma_{mt}\ V_m + \alpha_o\ \alpha_l\ \alpha_b\ V_f \tag{12}$$

Where: α_o, α_l, and α_b are orientation, length efficiency, and bond efficiency factors, respectively. Then he returned to neglecting the matrix strength at ultimate load, justifying that due to tensile cracking.

$$\sigma_t = 2\ \tau_f\ (\frac{l_f}{d_f}) \tag{13}$$

Where τ_f is the fiber bond strength, and it depends on the three factors above:

$$\sigma_{ct}\ = 2\ \alpha_o\ \alpha_l\ \alpha_b\ \tau_f\ V_f\ (\frac{l_f}{d_f}) \tag{14}$$

The assumed value of the parameters are as follows:

α_o = 0.41 for uniformly distributed fibers

α_b = 1.0 for straight fibers

$$\alpha_l\ = 1 - \frac{\tanh\left(\frac{\beta L_f}{2}\right)}{\frac{\beta L_f}{2}} \tag{15}$$

$$\beta = \sqrt{\frac{2\pi G_m}{E_f A_f \ln\left(\frac{s}{r_f}\right)}} \tag{16}$$

$$s = 25\ \sqrt{\frac{l_f}{V_f d_f}} \tag{17}$$

Where: G_m is the shear modulus of concrete matrix, l_f is steel fiber length. E_f, A_f, s, r_f, V_f are elastic modulus, cross-section area, average spacing, radius, and fiber volume fraction, respectively.

The flexural capacity is derived as follows:

$$M_n = A_s f_y \left(d - \frac{a}{2}\right) + \frac{\sigma t}{2} b(h-c)(h+c-a) \quad (18)$$

In which c is the depth of the neutral axis from extreme compression fiber and is calculated as follows:

$$c = \frac{A_s f_y + \sigma_t\, b\, h}{0.85 f'_c \beta_{1*} b + \sigma_t b} \quad (19)$$

Oh [6] found that the crack width was directly proportional to the steel stress and inversely to the fiber content. Also, the load capacity, flexural strength, and tensile strength increased by 50 %, 60 %, and 200 %, respectively, when fiber content was 2 %.

Khalil and Tayfur [7] proposed the same set of Oh equations [6] with some moderated and concluded values. They also neglected the matrix tensile strength and considered the same parameters for fibers as the ones considered by Oh. The modified values were bond efficiency factor of fibers = 1.2 instead of 1.0 due to using hooked and crimped fibers, while other factors remained the same.

The average fiber bond strength (σ_t) is moderated to be $\sigma_t = \tau_f \left(\frac{l_f}{d_f}\right)$ instead of $\sigma_t = 2\ \tau_f \left(\frac{l_f}{d_f}\right)$ that Oh used. They justified that the mean fiber pullout length is (l_f/4) instead of (l_f/2). The fiber tensile strength (by Khalil and Tayfur) was concluded as follows:

$$\tau_f = 0.66 \sqrt{f'_c} \quad (20)$$

The value of f'_c is assumed to be 136 MPa; therefore, the value of τ_f = 7.7 MPa, α_b=1.2, and the length efficiency factor =0.85. These values led to the tensile strength of fibrous concrete to be as follows:

$$\sigma_t = 0.85\ V_f\, \tau_f \left(\frac{l_f}{d_f}\right) \quad (21)$$

Al-Hassani et al. [8] derived an equation for predicting the flexural capacity of UHPC rectangular beam, considering a bi-linear relation for compression stress-strain diagram. The bi-linear compression stress-strain consisted of linear behavior up to 0.9 f'_c and the constant stress of 0.9 f'_c as perfect plastic behavior up to 1.5 ε_o (where ε_o is the strain at f'_c). Elastic-perfect plastic relation was also considered to imitate the tensile behavior of UHPC for analysis and design of flexural strength. Their equation was based on equilibrium conditions inside the cross-section of the beam. The derived equation was as follows;

$$Mn = 0.45\ f'_c\, b \left(c^2 - \frac{x_{c1}^2}{3}\right) + 0.5 f_{te}\, b \left(h^2 + c^2 - 2hc - \frac{x_{t1}^2}{3}\right) + A_s\, f_y\, (d - c) \quad (22)$$

Where; x_{c1} = the dimension of triangle length of the bi-linear compression relation, mm

x_{t1} = the dimension of triangle length of the bi-linear tensile relation, mm

f_{te} = the tensile stress at the end of the linear portion of bilinear relation, MPa, as shown in Figure 3.

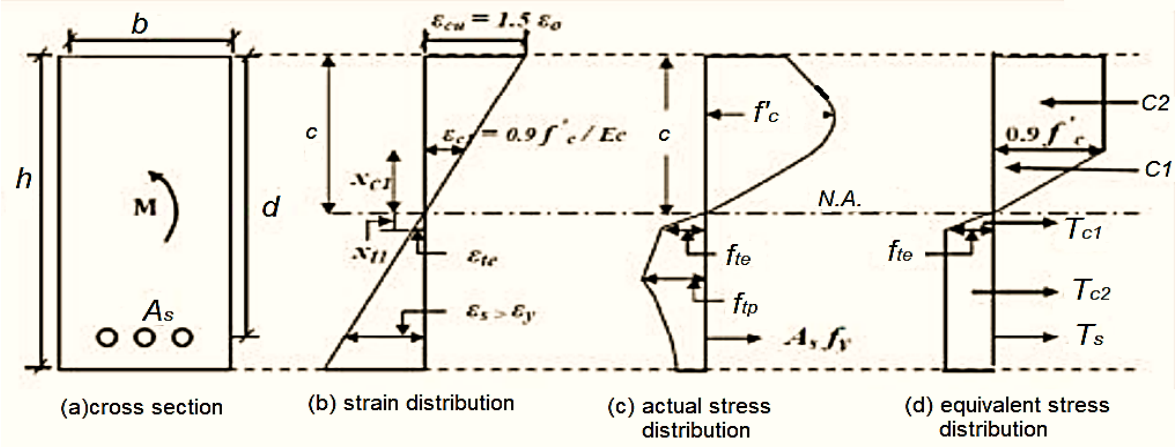

Figure 3: Actual and equivalent distribution of stress in UHPC rectangular cross-section at ultimate state [8]

Rasheed and Agha [9] proposed a set of equations to estimate the flexural capacity and balance reinforcement ratio. They considered a simplified rectangular block for compressive and tensile stresses. The flexural strength, according to their equation, consisted of steel rebar contribution and fibrous concrete contribution, as illustrated below;

$$Mn = As\ fy\ (d - \frac{a_f}{2}) + \sigma_{fu}\ b\ (h - \frac{a_f}{\beta_f})\ (\frac{h}{2} - \frac{a_f}{2} + \frac{a_f}{2\beta_f}) \quad (23)$$

Where; a_f = depth of equivalent compression zone for fibrous concrete, mm .σ_{fu} = tensile strength of fibrous concrete, MPa β_f = stress block parameter.

2. Analysis and Design Concepts of UHPC

The analysis and design philosophy of laterally loaded beams depends on the bending theory assumptions concerning the linear behavior in compression. Ultra high-performance concrete (UHPC) exhibits linear and non-linear behavior. It has a linear behavior up to 80% of its compressive strength, besides having strain hardening before reaching the compressive strength and strain softening after cracking, as illustrated in Figure 4. This behavior awards the ductility for UHPC when a failure occurs. On the other hand, UHPC is characterized by elongated strain before fracture in compression and during cracking in tension due to the existence of steel fibers. Also, it has high tensile strength compared to conventional concrete. Thus, it cannot be neglected when analyzing the beams for flexure and shear [10].

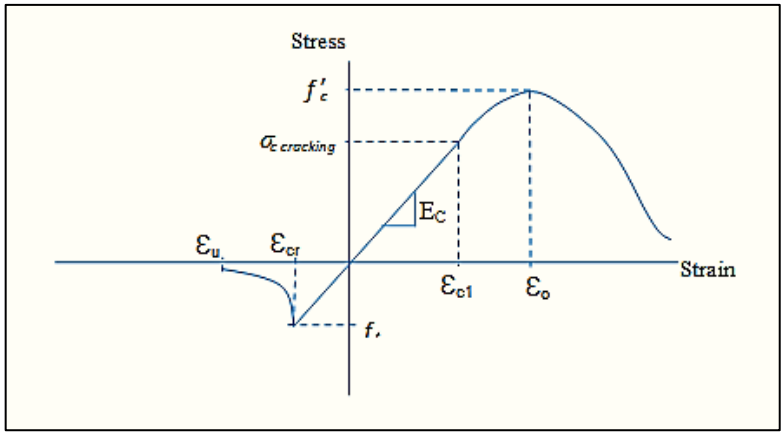

Figure 4: Compressive and Tensile Stress and Strain in UHPC

The behavior of UHPC beams reinforced with fibers and steel rebars is affected by some characteristic features. These are the high compressive strength, and relatively high tensile and flexural strengths, compared with NSC and HSC, besides the presence of fibers.

The orientation and distribution of fibers affect the tensile and flexural strength, which, in turn, improve the shear resistance. In addition, the fibers' orientation and uniform distribution relate to the mixing and pouring methods. Therefore, high-quality control is required for manufacturing UHPC.

For design UHPC members, many difficulties may confront the designers. The first is that tests are performed on small controlled specimens, and their behavior may differ from that of full-scale members because of geometry differences. Also, the orientation and distribution of fibers in small samples are controlled, while full-scale members are not. Therefore, conversion factors should be used in designing full-scale members [11].

The enhanced tensile and flexural strength of UHPC cannot be ignored as in conventional concrete. Hence, it must be considered in determining the flexural capacity of the beam.

The design recommendations must specify the principles wanted by the structural members. The first technical recommendation for using UHPC in construction was introduced in France in 2002 by AFGC. Then, a state-of-art report was presented in Germany in 2003 (DAfStb 2003). Next, the Japanese Society of Civil Engineers (JSCE) published design recommendations for UHPC in 2004. Finally, in 2012, Korea Concrete Institute (KCI) introduced a design code for UHPC [12].

It is more important to notice that a much lower ductility index is acquired when using steel rebars with a fibrous mixture. Yoo and Yoon [12] justified that due to the very high bond force between steel bars and UHPC and the crack localization behavior. Thus, the steel bars ruptured at a low mid-span deflection compared with UHPC beams without fibers.

2.1 DAfStb Guideline for UHPC

The German Committee for Structural Concrete (DAfStb) aimed to publish a guideline for UHPC in 2003. The Guideline contains two parts, one for the design of the building and civil engineering constructions that use UHPC with steel fibers, and the other for concrete technology and quality control of UHPC [13].

2.1.1 Stress-strain curve in compression for the design

The structural analysis depends on the stress-strain relationship in compression and tension for UHPC. The relatively high tensile strength and the post-cracking tensile strength, called nominal axial tensile strength of concrete, are transferred by fibers in the cracked state in the structural analysis and design process. For this reason, the design equations used for conventional concrete are modified or extended to consider the contribution of fibers [13].

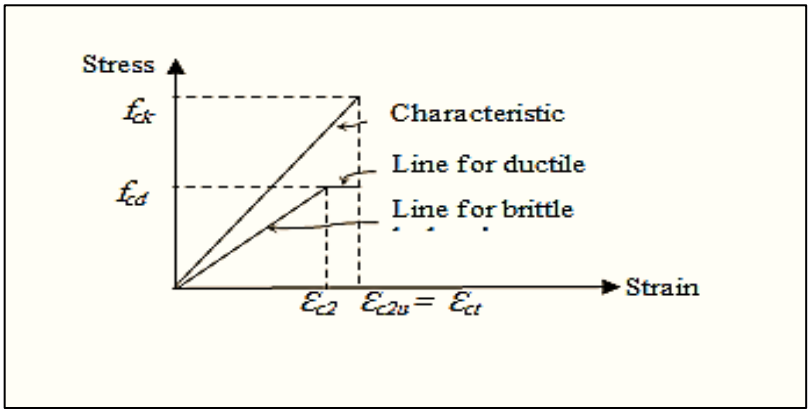

Figure 5: Stress-Strain Diagram for UHPC Under Compression

The stress-strain relationship of UHPC under compression is assumed to be linear and elastic up to the ultimate compression strength. As illustrated in Figure 5, the low nonlinear portion, which represents about (10-15) % of concrete compression strength, is neglected [11].

The design value of concrete compression strength (fcd) is:

$$f_{cd} = \frac{\alpha_{cc} f_{ck}}{\gamma_c \gamma'_c} \quad (24)$$

Where f_{ck} = characteristic value of cylinder compression strength.
γ_c γ'_c= safety factor for UHPC, their value range between (1.2-1.35)
α_{cc} = conversion factor between cylinder compression strength and member compression strength.
α_{cc} = 0.85 for long-term loading and creep effects
= 0.95 for short-term loading.
The design elastic modulus (E_{cd}) is given by:

$$E_{cd} = \frac{Ecm}{1.3} \quad (25)$$

E_{cm} is the mean value of elastic modulus. The compression strain at maximum loading (ε_{c2}) is given by:

$$\varepsilon_{c2} = \frac{fcd}{Ecd} \quad (26)$$

ε_{c2} is used when UHPC is without fibers or little fiber content, i.e., when the brittle behavior dominates. However, when fiber content is relatively high, the softening behavior occurs, and it must be considered in the design to represent the post-peak strain beyond ε_{c2}. Therefore, a plastic strain is represented by a horizontal line after ε_{c2} in Figure 5, which is added to express the ductile post-peak behavior [11].

The strain at the end of the plastic region is expressed as follows:

$$\varepsilon_{c2u} = \varepsilon_{c1} = \frac{fck}{Ec} \quad (27)$$

The plastic strain portion in the stress-strain relation does not represent the actual behavior of UHPC. Therefore, the stress-strain curve is moderated as illustrated in Figure 6, in which a linear decreased portion of strain-softening appears to reflect the ile behavior.

The linear elastic-linear softening stress-strain curve can also be moderated to a bilinear elastic-comparable plastic line, representing the internal compression forces [11].

According to Fehling et al. [11], the value of ε_{c2} = 0.0026, while the ultimate strain at ultimate compression strength, ε_{c2u} = 0.0035, which are maintained constant as for NSC and HSC [11,12].

2.1.2 Tensile stress-strain curve for the design

The contribution of fibers in the tensile strength of UHPC is more significant than in compressive strength. This contribution can be recognized at the onset of cracking. Therefore, it is important to distinguish between uncracked and cracked cases. The cracked case is postulated to the ultimate limit state analysis in which the tensile strength of UHPC without fibers is neglected as in conventional concrete. However, UHPC with fibers exhibits tensile strength, which should be included in the analysis and design flexural capacity.

The stress-strain curve in tension is represented by ascending curve up to ultimate tensile strength at which cracks are initiated, followed by a descending line representing the softening strain, as illustrated in Figure 7 [11, 14].

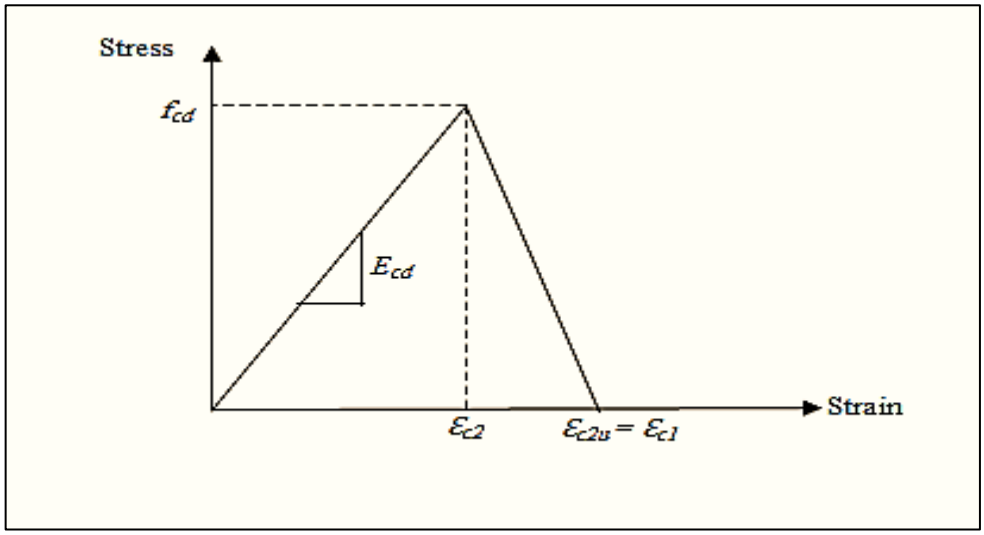

Figure 6: Stress-Strain Diagram for UHPC Under Compression

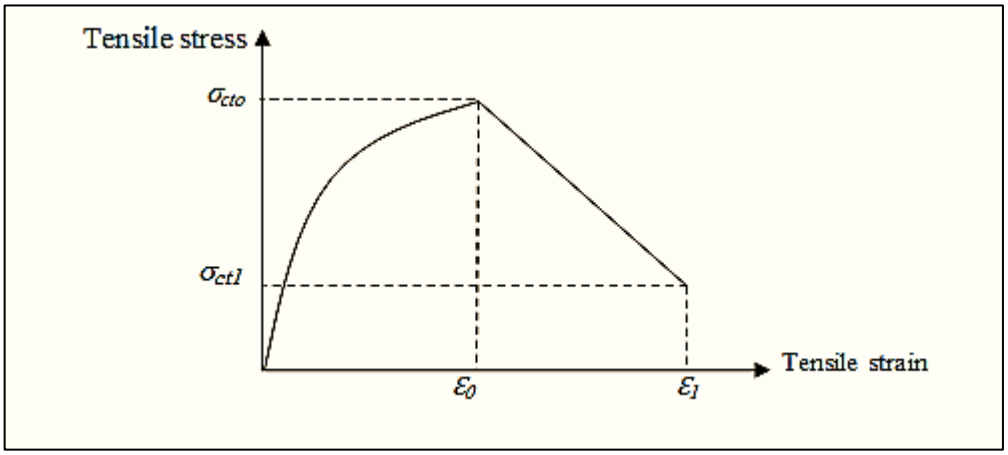

Figure 7: Stress-Strain Diagram for Cracked UHPFRC Under Tension

2.1.3 Design for flexural and axial force

The linear-elastic portion of the stress-strain curve in compression is assumed to visualize the compression action in the beam cross-section. The small plastic portion of ductile behavior is neglected due to its small value. In the tensile region under the neutral axis of the cross-section, the stress-strain curve in tension represents the tensile stress of concrete reinforced by fibers. In addition, the tensile stress of reinforcing bars is used in the beam [11,13].

Figure 8 visualizes the assumed distribution of stresses and the internal forces used in the flexural design of beams [13].

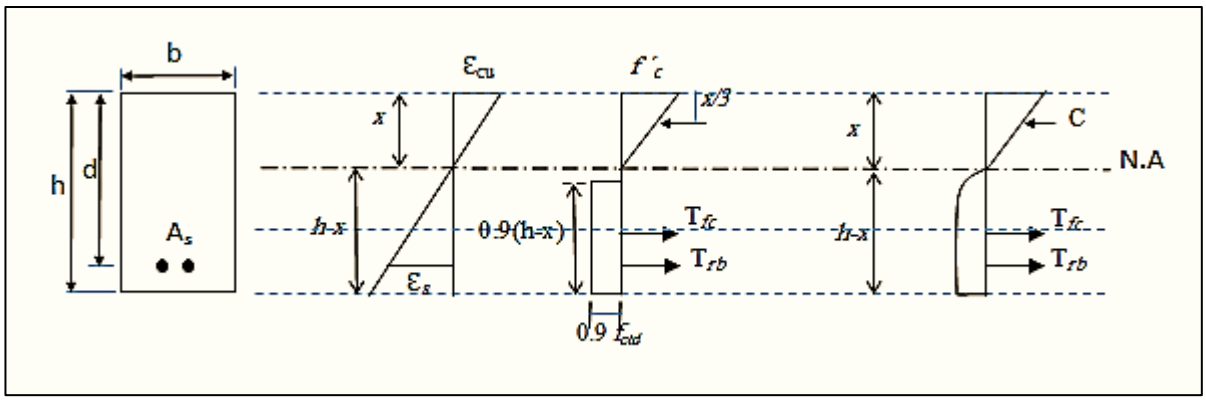

Figure 8: Stress and Strain Distribution for The Flexural Design of Beam

The compression force in concrete and the tensile force in the rebar, besides the tensile force in concrete under the neutral axis are found as follows;

$$C = \frac{1}{2} b \, x \, f'c \tag{28}$$

$$T_{rb} = As \, fy \tag{29}$$

$$T_{fc} = 0.81 \, b \, (h\text{-}x) \, \sigma_{ctd} \tag{30}$$

The neutral axis can be found by using strain compatibility and equilibrium conditions. Also, equilibrium conditions are used to find the internal forces and moment capacity [15].

$$C = T_{fc} + T_{rb} \tag{31}$$

$$M = C \, (d\text{-}x/3) + T_{fc} \, (d\text{-} \, 0.45 \, x - 0.55 \, h) \tag{32}$$

2.2 AFGC-SETRA Recommendations for UHPC

The French Civil Engineering Association (AFGC) 2002 issued recommendations on UHPFRC, the first issue on this new cementitious material. According to Ductal's mechanical test findings, the parameters to structural design were assigned as follows: f′c =150-250 MPa, f_{tj} = 8 MPa and Ec=55 GPa, where f_{tj} is the post-cracking direct tensile strength [12]. The assumptions that are depended on in determination the ultimate moment capacity in the ultimate limit states are as follows [15]:

- Plane sections remain plane after deformation obeying elastic limits.
- The compression strain in UHPFRC shall be limited to Ɛcud, and the strains in reinforcing steel shall be limited to Ɛud, as shown in Figure 9.

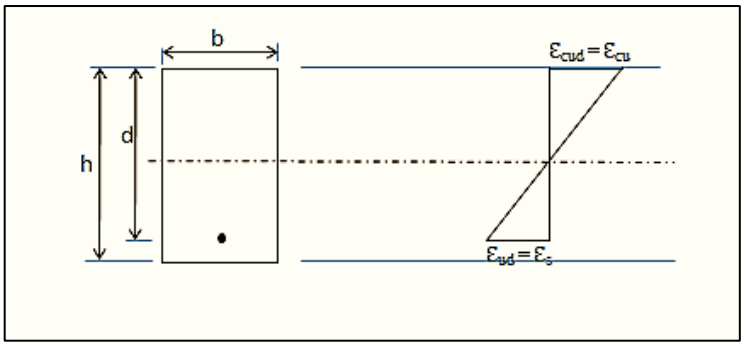

Figure 9: Diagram of Relation Deformations at ULS

AFGC considered the effect of fiber orientation which was represented by the K-coefficient. K-coefficient is used to consider the differences between fiber orientation in structure from that in prism specimen, its value equal to or greater than 1.0 [16].

A bilinear stress-strain mode is used for compression with a maximum value of compression strain = 0.003. The tensile stress-crack width pattern is used in the inverse analysis, which is transformed into a tensile stress-strain pattern using a characteristic length, *lc*. $lc = \frac{2}{3}$ h for rectangular or T-beams, in which h is the overall height of the beam [12].

To attain the tensile stress-strain pattern, it is required to calculate the elastic tensile strain of 0.3 mm and crack width strain of 0.01h, using the following equations [12,15]:

$$Ɛe = \frac{fti}{Ec} \tag{33}$$

$$Ɛ_{0.3} = \frac{w0.3}{lc} + \frac{f_{ti}}{\gamma_{bf} E_c} \tag{34}$$

$$Ɛ_{0.01} = \frac{w0.01}{lc} + \frac{f_{ti}}{\gamma_{bf} E_c} \tag{35}$$

In which; Ɛe = elastic strain
$w_{0.3}$ =the crack width of 0.3 mm
$Ɛ_{0.3}$ = strain at crack width of 0.3 mm
$w_{0.01}$ = the crack width of 0.01h
$Ɛ_{0.01}$ = strain at crack width of 0.01h.

The ultimate tensile strain:

$$\varepsilon e = \frac{lf}{4lc} \tag{36}$$

Where l_f is the length of the fiber. The following equations are used to calculate the stresses at $w_{0.3}$ and $w_{0.01}$:

$$f_{bt} = \frac{f(w_{0.3})}{K\gamma_{bf}} \tag{37}$$

$$f_{1\%} = \frac{f(w_{0.01})}{K\gamma_{bf}} \tag{38}$$

Where f_{bt} represents the stress at 0.3 mm crack width and $f_{1\%}$ is the stress at crack width of 0.01h.
K =1.0 when fiber orientation coincides in both the specimen and structure.
K =1.25 when loads differ from local effects.
K =1.75 for local effects.
γ_{bf} refers to a partial safety factor under tension.
γ_{bf}= 1.30 for essential combination effects which require fiber sharing in very localized areas.
γ_{bf}= 1.05 for accident combination effects [12,15].

AFGC distinguished two formulations for tensile behavior. The first is the strain-softening formulation when fti > fbt, and the second is the strain hardening formulation when fti < fbt, where fbt is the tensile stress at 0.3 crack width is defined by equation (37). Figure 10 depicts the stress-strain diagram under compression and tension.

According to the direct tensile behavior, AFGC identified three types of UHPFRC as follows [14]:
Type I: strain-softening can be used for thin and thick structures.
Type II with slightly strain hardening is also used for both thin and thick structures.
Type III with strain hardening is used for thick structures.

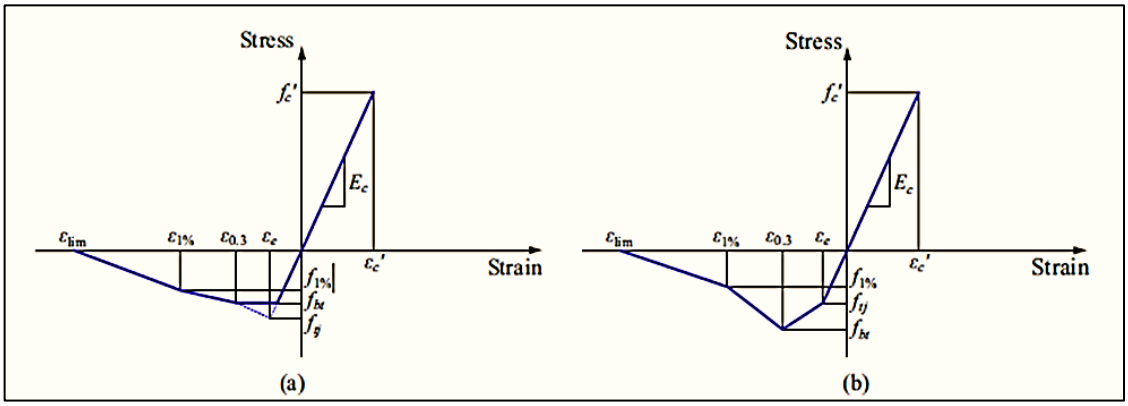

Figure 10: Stress-Strain Diagram of Material Pattern, (a) Strain Hardening, (b) Strain Softening

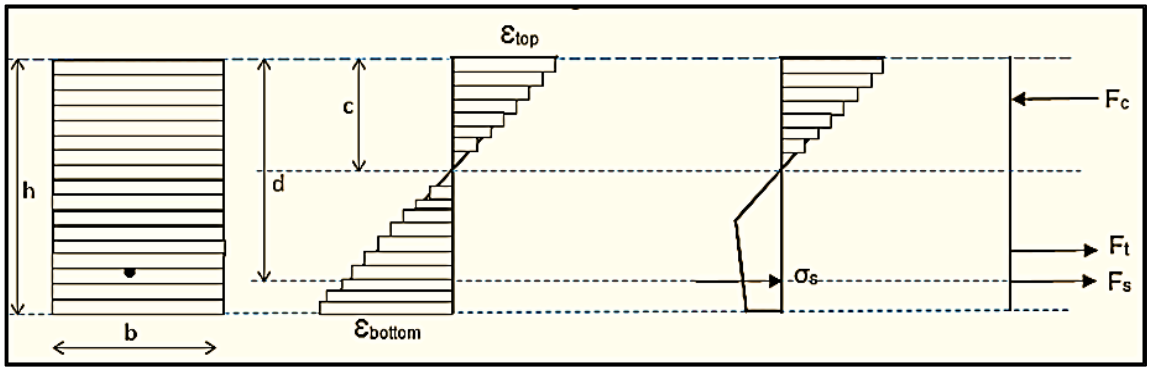

Figure 11: Beam Cross-Section with Strain and Stress Action

The beam cross-section subjected to bending can be described in Figure 11 [12,17]. The flexural design of UHPFRC members is not present in the AFGC recommendations [17].

2.3 Japan Society of Civil Engineers (JSCE) Recommendations

The following symbols are used in the JSCE Recommendations for UHPFRC:
f'_c is the compressive strength ≥ 150 MPa; f_{crk} is cracking strength ≥4 MPa
f_{tk} is tensile stress at a crack width of 0.5 mm; w_k is crack width
γ_c is a partial safety factor; l_{ch} is characteristic length, and G_f is fracture energy.

JSCE Recommendations used a Ductal mixture with heat treatment and steel fibers with a volume fraction of 2 %, diameter of 0.2 mm, and length of 15 mm. The structural analysis and design based on f'_c =180 MPa, f_{crk}=8 MPa, Ec= 50 GPa and γ_c =1.3.

The bilinear stress-strain curve is assumed for compression, and the bilinear curve for tension-crack width represents the tension softening, as shown in Figure 12 [17].

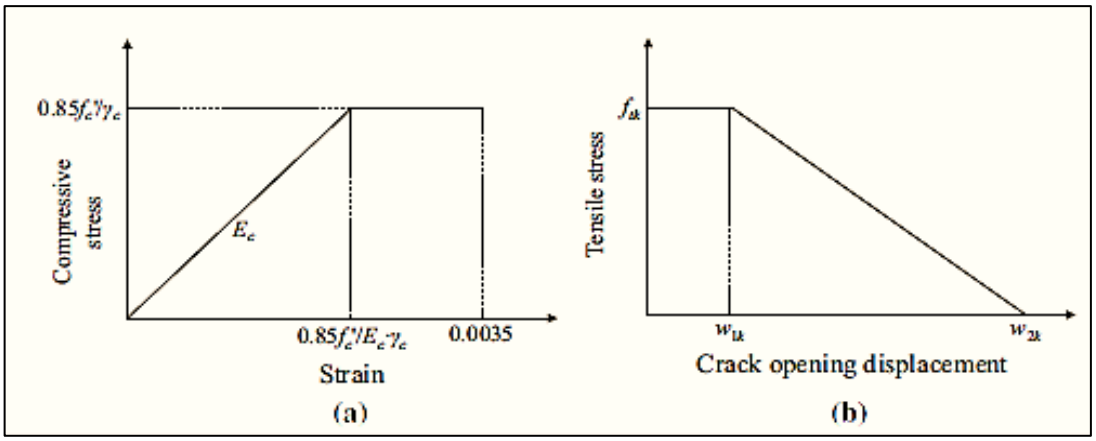

Figure 12: Material models [JSCE recommendations (JSCE 2004)]; a) compressive stress–strain curve, b) tension-softening curve

The bilinear tension softening is transformed into the stress-strain curve with the tensile stress in the cross-section. The crack width must be transformed to strain, using the equivalent specific length l_{eq} as follows [12]:

$$l_{eq} = 0.8\ h\ (1- \frac{1}{\left(1.05+\frac{6h}{L_{ch}}\right)^4}) \quad (39)$$

Where h is the total depth of the beam and l_{ch} is the characteristic length and calculated as follows:

$$l_{ch} = \frac{G_f E_c}{f_{tk}^2} \quad (40)$$

The tensile stress-strain pattern can be found as follows:

$$\text{Factored elastic strain: } \varepsilon_{cr} = \frac{f_{tk}}{\gamma_c Ec} \quad (41)$$

$$\text{Strain at 0.5mm crack width: } \varepsilon_1 = \varepsilon_{cr} + \frac{w_{1k}}{leq} \quad (42)$$

$$\text{Strain at 4.3mm crack width: } \varepsilon_2 = \frac{w_{2k}}{leq} \quad (43)$$

Some assumptions are affixed by JSCE to be satisfied for structural design. These assumptions conclude linear strain distribution, using compressive stress-strain pattern and tensile stress-crack width pattern as shown in Figure 12 above. But JSCE does not contain a detailed procedure for determining the ultimate flexural capacity [12]. However, equilibrium conditions and compatibility of strains can be applied to do so.

2.4 Khalil and Tayfur Equations of Moment Capacity

Based on ACI 318M-11[4] and the proposed equation for predicting the nominal moment capacity of fibrous reinforced concrete, Khalil and Tayfur introduced two sets of equations to calculate the nominal flexural capacity of singly reinforced UHPC beams with full depth and half depth fibers reinforced UHPC. Figure 13 depicts the strain and stress distribution throughout the cross-section of the rectangular beam [7].

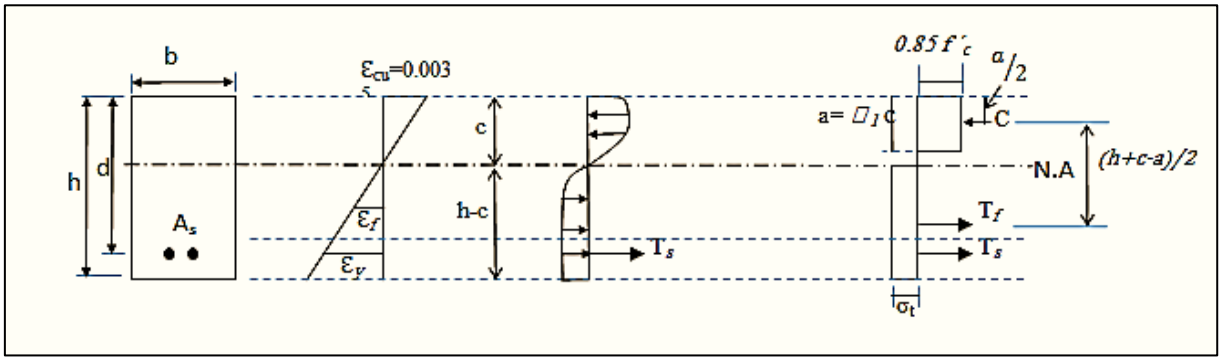

Figure 13: Compressive and Tensile Stress and Strain of Fibrous UHPC Concrete [7]

$$\text{For full depth UHPC; } M_n = As\ fy\ (d-\ a/2) + \frac{\sigma t}{2}\ b\ (h\text{-}c)\ (h+c\text{-}a) \tag{44}$$

$$a = \frac{As\ fy + \sigma t\ b\ h}{\lambda\ f'cf + \sigma t\ b} \tag{45}$$

Where, f'_{cf} is compressive strength of fibrous UHPC

$$\text{For half depth UHPC; } M_n = A_s\ f_y\ (d-\ a/2) + \frac{\sigma t}{8}\ b\ h\ (3h\text{-}2c) \tag{46}$$

$$a = \frac{As\ fy + \sigma t/2(\ b\ h)}{\lambda\ f'c\ b} \tag{47}$$

2.5 Pourbaba et al. Proposed Method to Predict UHPC Flexural Capacity

Pourbaba et al. [18], based on Yoo and Yoon's [17] investigations, tested ten UHPFRC beams using two types and lengths of steel fibers, 13 mm smooth and 30 mm twisted fibers, well as two reinforcement ratios, 0.94 and 1.5 %. Their results showed that the length and type of fibers did not significantly affect the compressive strength and elastic modulus, whereas they highly enhanced the flexural strength. Also, they noticed that the longer fibers have more effective post-cracking stiffness and capacity than shorter fibers.

Pourbaba et al. [18, 19] clarified that, despite the availability of some recommendations for the AFGC, JSCE, ACI 544.4R, and DAfStb at present, there is no unified method for designing the flexural capacity of UHPC beams. They studied some of the available equations and compared them with experimental results. Then, they selected the equations that they considered to be utilized for predicting the moment capacity, as follows:

$$\text{The elastic modulus, } E_c = 11800\ (f'_c)^{\frac{1}{3.14}} \tag{48}$$

$$E_c = 3755\ \sqrt{f'_c} \tag{49}$$

To calculate the limited tensile strength of UHPC, f_{tu}, which represents the cracking tensile stress, the equation derived by Wille et al. [20] is selected.

$$f_{tu} = 7.5 + \alpha_t\ V_t\ (\frac{lf}{df}) \tag{50}$$

The 7.5 represents the matrix tensile strength, and αt is a coefficient related to fiber orientation and the bond behavior before cracking, including adhesive component and friction. The value of αt is 0.01, 0.03, and 0.025 for hooked, straight, and twisted fibers, respectively [20].

The equation derived by Khalil and Tayfur [7] and Oh [6] is considered to calculate the flexural capacity, Mn of UHPC beams.

$$Mn = As\ fy\ (d-\ a/2) + \frac{\sigma t}{2}\ b\ (h\text{-}c)\ (h+c\text{-}a) \tag{51}$$

The depth of neutral axis, c is found as follows [16];

$$c = \frac{As\ fy + \sigma t\ b\ h}{0.85\ f'cf\ \beta 1\ b + \sigma t\ b} \tag{52}$$

Where β_1 is a factor related to compressive strength. When compressive strength exceeds 30 MPa, β_1 decreases linearly at 0.7 per 7 MPa, but it must not be less than 0.65. i.e.

$\beta 1 = [0.85 - 0.07(f'c - 30)]/7 \geq 0.65$ (as it is limited in ACI 318-M Code), f'cf is the compressive strength of fibrous concrete [7, 19].

The tensile strength, σt, is calculated as follows;

$$\sigma t = 2\ \alpha_o\ \alpha_b\ \alpha_l\ V_f\ \tau_f\ (\frac{lf}{df}) \quad (53)$$

This equation was derived previously by Oh [6] for fiber-reinforced concrete.

However, α_o is a factor of fiber orientation, αb is a bond efficiency factor between steel fibers and concrete, where;

α_o =0.41 for concrete with uniformly distributed fibers

α_b = 1.0 for straight fibers

= 1.2 for waved or hooked fibers,

α_l is a factor of fiber length and is calculated as follows;

$$\alpha_l = 1 - \frac{\tanh\left(\frac{\beta L_f}{2}\right)}{\frac{\beta L_f}{2}} \quad (54)$$

β is a parameter calculated as follows;

$$\beta = \sqrt{\frac{2\pi G_m}{E_f A_f \ln\left(\frac{s}{r_f}\right)}} \quad (55)$$

Where s is the average spacing between steel fibers, and is calculated as follows:

$$s = 25\sqrt{\frac{lf}{Vf\ df}} \quad (56)$$

All these parameters and factors were derived previously by Oh [6].

$$\tau_f = 0.66\sqrt{f'_c} \quad (57)$$

Which was redacted previously by Hanger and Doherty as reported in ACI 544.4R [3] and mentioned by Khalil and Tayfur [7].

The distance of the neutral axis from the extreme compression fiber is found as it is given in ACI 318-M Code as follows;

$$c = a\ /\ \beta_1 \quad (58)$$

Pourbaba et al. also refer to the equations proposed by Campione [21]. They depended on these equations to find the ultimate moment capacity, Mu.

Another equation to find the position of neutral axis, which Campione proposed, is depended as follows:

$$c = \frac{\rho d\ fy + fr\ h}{0.68\ f'c + fr + 333.3\frac{fr\ ft}{Ect}} \quad (59)$$

Where ρ is the ratio of reinforcement = As/bd, d is the effective depth from extreme compressive fiber to centroid of reinforcing bars, h is the overall height of cross-section, and f_r is the strength of fibrous concrete in tension which is calculated as follows:

$$fr = 0.3\ F\ \tau \quad (60)$$

$$\tau = 0.66\sqrt{f'_c} \quad (61)$$

$$F = \gamma\ V_f\ (\frac{lf}{df}) \quad (62)$$

Where ɣ is the bond efficiency factor = 0.5 for round fibers.Campione [21], introduced another formula for strength of fibrous concrete in tension, fr which was proposed by Foster and Attard [21], as follows:

$$fr = 0.375\ F\ \tau \quad \text{(in MPa)} \quad (63)$$

The distance from the extreme compression fiber to the top of the tensile stress block of fibrous concrete e is given as follows:

$$e = \frac{c}{0.003}\left(\frac{ft}{Ect} + 0.003\right) \quad (64)$$

Finally, the ultimate moment capacity, Mu, is calculated by the following equation:

$$Mu = b\,d2\left[\rho\, fy\,(1-0.4\,\frac{c}{d}) + fr\,(\frac{h-e}{d})(\frac{h}{d} - \frac{h-e}{2d}) - 0.4\,\frac{c}{d}\right] \quad (65)$$

According to some equations reported by researchers, a comparison between the experimental moment capacity with the theoretical one showed that all these equations underestimated the experimental values [19]. That means high conservation was taken by researchers when deriving these equations.

Pourbaba et al. showed that the UHPC failure mode depended on the reinforcement ratio. For high ratios, shear-flexure mode governs, while flexure mode governs for low reinforcement ratios.

3. Shear behavior of Reinforced Concrete Beams

3.1 Shear Resistance of Ordinary Reinforced Concrete Beams

When a simple beam is subjected to lateral loading on one face, bending moment and shear force initiate at any section to maintain that section's equilibrium according to the materials' mechanics. The bending moment causes compression stresses in the concrete portion above the neutral axis and tensile stresses in the reinforcement bars and the concrete below the neutral axis. This is the case for the uncracked section, as shown in Figure 14.

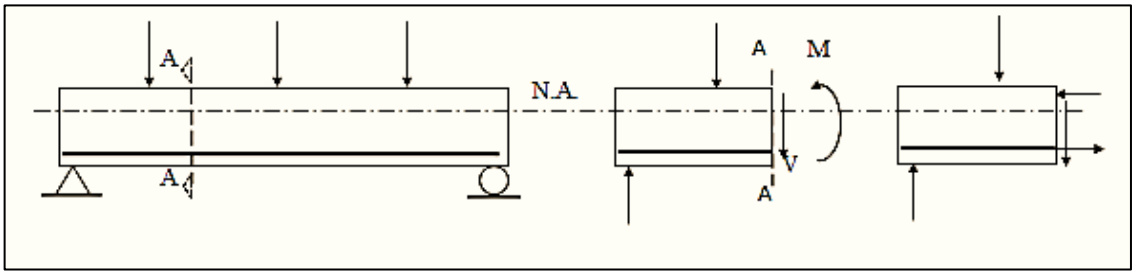

Figure 14: Shear Force and Bending Moment in A Simply Supported Beam

For any element in the beam, shear, tensile and/or compression stresses act on its faces, depending on the element's location concerning the neutral axis. For example, the element located at the neutral axis is subject to a pure shear state, leading to principal tensile stress acting on an inclined plane at a 45^0 angle. As depicted in Figure 15, this principle of tensile stress represents diagonal tension that causes diagonal cracking and leads to shear failure of the beam before reaching ultimate flexural strength. Therefore, the failure of beams is commonly shear failure rather than flexural failure [1].

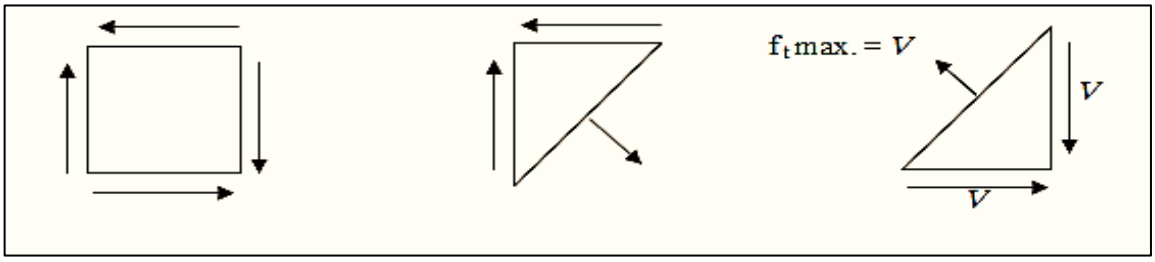

Figure 15: Pure Shear State on an Element at N.A

According to the equilibrium, the maximum shear stress at the neutral axis is given by the equation:

$$v_{max.} = \frac{V}{b\,d} \quad (66)$$

Where V is the vertical shear force at the section, kN; b is the width of the cross-section; and d is the effective depth of the cross-section.

In the beam section, where the flexural stress is small near the supports in simply supported beam or where flexural cracks exist, the stress condition is nearly the state of pure shear, which causes equality of inclined tensile stress at 45^0 with the shear stress.

The flexural stress is no longer linear in the compression zone. Thus the inclined principal tensile stress is not the actual tensile stress. However, it is assumed to measure the potential of inclined cracking [1].

3.2 The Behavior of RC Beams Without Shear Reinforcement Under Shear Action

The behavior of RC beams under loading varies widely depending on the load intensity and some other factors. However, the beam under loading exhibits a variate mechanism to transfer the shear throughout the section, whereas the common shear failure in a beam without shear reinforcement is brittle. Generally, the mechanisms of shear transfer in RC beam can be depicted as shown in Figure 16 and illustrated as follows [1,22];

Shear force at compression zone of concrete, V_c.

Interface shear transfer along with the diagonal cracking (aggregate interlock), V_a

Dowel action at the level of longitudinal reinforcement, V_d.

Arch action in deep (short) beams

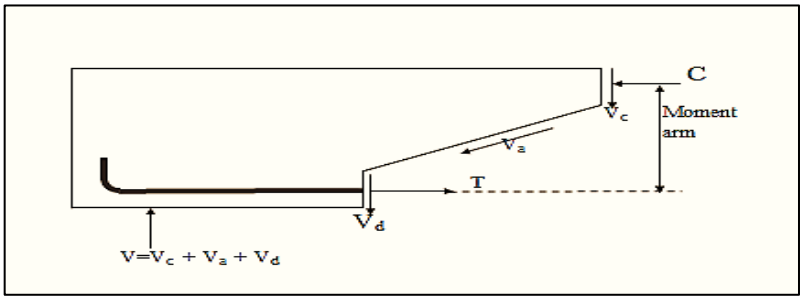

Figure 16: Shear Components After Formation of Cracks

Shear stress in beams leads to inclined cracks in the web. Inclined cracks that occur in the web without previous flexural cracks are known as web-shear cracks, while the inclined cracks that propagate beyond flexural cracks are known as flexure-shear cracks. Flexural cracks are somewhat vertical on the bottom face of the beam and refer to as initiating cracks [1].

Chana [22] studied the mechanism of shear failure in RC beams. She proposed that flexural cracks initiate at the bottom face of the beam firstly, at intervals depending on the reinforcement ratio (ρ_w) and the depth of cross-section (d). the flexural cracks rise to a short distance, then deviate from the vertical direction towards the mid-span position due to shear stress-induced. The inclination of these cracks increases when they go towards supports. The shear force is restricted by the compression zone of concrete, diagonal interface shear, and dowels to some extent. When the applied shear force increases, the diagonal cracks widen, leading to increased dowel action. Then, splitting cracks along the reinforcement bars occur due to loss of bonding accompanied by a redistribution of stresses along the dowel cracks. Finally, the dowel cracks increase rapidly and widen with the increase of loading, causing failure. Ghana attributed the failure due to the loss of dowel forces. When dowel cracking initiates, the restraint between the bar segment and both sides of diagonal cracking is lost to cause failure.

In general, the beam's ability to sustain further loading after the formation of inclined cracks depends on its ability to redistribute that loading across the inclined crack. All the three mechanisms described above can participate in the redistribution.

Other factors are influenced the shear capacity. For example, Yaseen [23] showed that the compression strength and reinforcement ratio increased the ultimate shear capacity, whereas raising the a/d ratio decreased Vu. Also, increasing compression strength caused increasing diagonal crack-load.

For RC beams without shear reinforcement, after propagation of crack up and in an inclined direction, the shear transfer at various proportions by the mechanisms as follows; 15-20 % by dowel action; 20-40 % by uncracked concrete in compression zone and 33-50 % by interface diagonal shear. This proportion of contribution varies with the increase in length and width of diagonal cracks, where interface shear transfer strength decreases with the lengthening and widening of diagonal cracks [22].

3.3 Mechanisms of Shear Failure in RC Beams

At the start of loading, the beam is free of cracks. At this stage, the whole section contributes to carrying the loads; therefore, the deflection is small on slightly increasing the load and is proportional to that load. Upon increasing load up to flexural cracking load, the first crack initiates at the tension region in the middle of the span to form flexural cracks, which extend up to the neutral axis position, accompanied by the increase of deflection. With further load increase, other flexural cracks initiate in both the center and shear span of the beam, then propagate differently. Where the cracks in the middle of the span propagate vertically, the shear span cracks diverge toward the position of applied load [24,25].

The number, size, and spacing of cracks differ with the longitudinal reinforcement ratio difference. The direction of flexural cracks continues upward until inclined shear cracks generate. Shear cracks are accompanied by the increase of strain in stirrups which give the ductile behavior of the beam.

In T-beam, shear cracks propagate at an inclination less than 45^0 upward to the flange and downward to the tensile reinforcement. At increasing load further, the bottom end of the shear crack propagates and extends along with the tensile reinforcement for a distance equal to at least the spacing between two adjacent stirrups. At the same time, the upper end of the crack reaches the bottom of the flange to extend horizontally with the extent of junction between flange and web to a certain distance. Therefore, sudden failure occurs due to the crack extension across the flange toward the position of the applied load [24]. In rectangular beams, shear cracks propagate up toward the compression zone of concrete, increasing loading till failure [1]. For beams without shear reinforcement, the failure occurs shortly after initiation of shear crack [24]

As illustrated previously, UHPC with optimum packing density has a dense microstructure, which is the prime cause for its high strength and elastic modulus. Subsequently, it has high stiffness as compared with NSC and HSC. Unfortunately, the high strength causes unfavorable brittle failure of concrete. However, using high tensile strength fibers can overcome this deficiency. Furthermore, the use high strength steel fibers can improve the post-peak behavior in compression and tension, which is characterized by strain hardening, besides their contribution to increasing the tensile strength obviously and compressive strength slightly.

The very high compressive strength of UHPC leads to the design of structural members with smaller sizes and lightweight than the NSC or HSC under the same loading [26].

Maca et al. [27] pointed to Cavill and Chirgwin's vision, who stated that reducing 35 % of material quantity upon using UHPC compared with normal concrete has the same strength.

4. Conclusion

According to the approaches adopted to analyze the UHPC beams, the following conclusions can be drawn:

1) The main procedure used to determine the flexural capacity of the beam depends on the equilibrium of the sections for the forces that emerged on loading in compression and tension zones. In addition, the presence of fibers in UHPC increases the tensile strength and enhances the post-cracking behavior. Therefore, the tensile strength of UHPC should be considered in determining the flexural capacity of UHPC beams.
2) The structural analysis of UHPC depends on the stress-strain relationship in compression and tension. The linear portion of compression relation extends to about 80% of the compressive strength; therefore, it is considered in the analysis and design process.
3) The safety factor used for conventional concrete can also be used for UHPC in compression, whereas 80-90 % of tensile strength is considered.
4) The use of steel fibers in UHPC cannot fully substitute steel rebars to compensate for the weakness of concrete in tension, but it can reduce the percentage of reinforcements.
5) Adding steel fibers in a percentage greater than 2 % can partially replace shear reinforcement since it can enhance the shear capacity of the beam.

Author contribution

All authors contributed equally to this work.

Funding

This research received no specific grant from any funding agency in the public, commercial, or not-for-profit sectors.

Data availability statement

The data that support the findings of this study are available on request from the corresponding author.

Conflicts of interest

The authors declare that there is no conflict of interest.

References

[1] C.K. Wang, C.G. Salmon, J.A. Pincheria, Reinforced Concrete Design; seventh edition, John Wiley & Sons Inc. 2007.

[2] A. A. Abdulsada, R. I. Khalel, and K. F. Sarsam, Influence of Minimum Tension Steel Reinforcement on the Behavior of Singly Reinforced Concrete Beams in Flexure, Eng. Technol. J., 38 (2020) 1034–1046. https://doi.org/10.30684/etj.v38i7a.902

[3] ACI 544.4R88, Design Considerations for Steel Fiber Reinforced Concrete, American Concrete Institute, Detroit 1999.

[4] A. C. I. Committee, 318M-19: Building Code Requirements for Concrete and Commentary.

[5] M.I.M. Rjoub, Moment Capacity of Steel Fiber Reinforced Concrete Beams, J. Eng Sci. Assiut Univ., 34 (2006) 413-422. https://dx.doi.org/10.21608/jesaun.2006.110462

[6] B.H. Oh, Flexural Analysis of Reinforced Concrete Beams Containing Steel Fibers, J. Struct. Eng., 118 (1992) 2821-2835. https://doi.org/10.1061/(ASCE)0733-9445(1992)118:10(2821)

[7] W. I. Khalil, Flexural Strength of Fibrous Ultra High Performance, APRN J. Eng. Appl. Sci., 8 (2013) 200–214.

[8] H. M. Al-Hassani, W. I. Khalil, L. S. Danha, Prediction of the Nominal Bending Moment Capacity for Plain and Singly Reinforced Rectangular RPC Beam Sections Prediction, Eng. Technol. J., 33 (2015) 1113–1130.

[9] M. H. F. Rasheed, A. Z. S. Agha, Analysis of Fibrous Reinforced Concrete Beams, Eng. Technol. J., 30 (2012) 974–990.

[10] A. M. Jabbar, M. J. Hamood, and D. H. Mohammed, Ultra High Performance Concrete Preparation Technologies and Factors Affecting the Mechanical Properties: A Review, IOP Conf. Ser. Mater. Sci. Eng., 1058, 2021, 012029. https://doi.org/10.1088/1757-899x/1058/1/012029

[11] Fehling, E.; Schmidt, M.; Walraven, J.; Leutbecher, T.; Frohlich, S.; Ultra-High Performance Concrete, Fundamentals, Design, Examples, Beton Kalender, Wilhen Ernst and Sohn, Germany, 2014.

[12] D. Y. Yoo and Y. S. Yoon, A Review on Structural Behavior, Design, and Application of Ultra-High-Performance Fiber-Reinforced Concrete, Int. J. Concr. Struct. Mater., 10 (2016) 125–142. https://doi.org/10.1007/s40069-016-0143-x

[13] M. Schmidt, T. Leutbecher, S. Piotrowski, and U. Wiens, The German Guideline for Ultra-High Performance, UHPFRC 2017 Des. Build. with UHPFRC New large-scale implementations, Recent Tech. Adv. Exp. Stand. 2 (2017) 545–554.

[14] Simon, A. 2011. New AFGC Recommendations of UHPFRC: chapter 1- Mechanical Characteristic and Behavior of UHPFRC, Designing and Building with UHPFRC, State of the art and Development, edited by Francois Toutlemonde, Jacques Resplendino, John Wiley and Sons Inc, p.p.723-741. https://doi.org/10.1002/9781118557839.ch48

[15] French Standard Institute; National addition to Eurocode 2-Design of Concrete Structures: Specific Rules for Ultra-High Performance Fibre-Reinforced Concrete (UHPFRC), 2016.

[16] Pierre MARCHAND.. New AFGC Recommendations on UHPFRC: Chapter 2 – Design. Designing and Building with UHPFRC. State of the Art and Development. Edited by François Toutlemonde, and Jacques Resplendino. John Wiley & Sons, Inc,2011. https://doi.org/10.1002/9781118557839.ch49

[17] D. Y. Yoo and Y. S. Yoon, Structural performance of ultra-high-performance concrete beams with different steel fibers, Eng. Struct., 102 (2015) 409–423. https://doi.org/10.1016/j.engstruct.2015.08.029

[18] M. Pourbaba, H. Sadaghian, and A. Mirmiran, A comparative study of flexural and shear behavior of ultra-high-performance fiber-reinforced concrete beams, Adv. Struct. Eng., 22 (2019) 1727–1738, https://doi.org/10.1177/1369433218823848

[19] M. Pourbaba, H. Sadaghian, A. Mirmiran, Flexural Response of UHPFRC Beams Reinforced with Steel Rebars, Adv. Civ. Eng. Mater., 8 (2019) 20. https://doi.org/10.1520/acem20190129

[20] K. Wille, S. El-Tawil, A. E. Naaman, Properties of strain hardening ultra-high performance fiber reinforced concrete (UHP-FRC) under direct tensile loading, Cem. Concr. Compos., 48 (2014) 53–66. https://doi.org/10.1016/j.cemconcomp.2013.12.015

[21] G. Campione, Simplified flexural response of steel fiber-reinforced concrete beams, J. Mater. Civ. Eng., 20 (2008) 283–293. https://doi.org/10.1061/(ASCE)0899-1561(2008)20:4(283)

[22] P. S. Chana, Investigation of the mechanism of shear failure of reinforced concrete beams, Mag. Concr. Res., 39 (1987) 196–204. https://doi.org/10.1680/macr.1987.39.141.196

[23] S. A. Yaseen, An Experimental Study on the Shear Strength of High-performance Reinforced Concrete Deep Beams without Stirrups, Eng. Tech. J., 34 (2016) 2123–2139. https://doi.org/10.30684/etj.34.11A.17

[24] M. N. Palaskas, E. K. Attiogbe, and D. Darwin, Shear Strength of Lightly Reinforced T-Beams, 1982.

[25] R. Thamrin, J. Tanjung, R. Aryanti, O. F. Nur, and A. Devinus, Shear strength of reinforced concrete T-beams without stirrups, J. Eng. Sci. Technol., 11 (2016) 548–562.

[26] M. Baqersad, E. A. Sayyafi, H. Mortazavi Bak, State of the Art: Mechanical Properties of Ultra-High Performance Concrete, Civ. Eng. J., 3 (2017) 190–198. https://doi.org/10.28991/cej-2017-00000085

[27] P. Máca, R. Sovják, T. Vavřiník, Experimental investigation of mechanical properties of UHPFRC, Procedia Eng., 65 (2013) 14–19. https://doi.org/10.1016/j.proeng.2013.09.004